Conformational Properties of Adenylyl-3′→5′-adenosine in Aqueous Solution†

Norman S. Kondo‡ and Steven S. Danyluk*

ABSTRACT: A detailed 220-MHz NMR study has been made of the conformational properties for the homodinucleotide adenylyl-3′→5′-adenosine, ApA, in D_2O. Unambiguous signal assignments of *all* proton signals were made with the aid of selectively deuterated nucleotidyl units, *ApA, Ap*A, and D-8ApA, and complete, accurate sets of NMR parameters were derived by simulation-iteration methods. Sets of limiting chemical shifts and coupling values were also obtained for ApA and constituent monomers 3′-AMP and 5′-AMP at infinite dilution and at identical ionization states for assessment of dimerization effects. Conformational properties were evaluated quantitatively for most of the conformational bonds of ApA and these are consistent with two compact folded dynamically averaged structures, a base-stacked right helical structure, I, characterized as anti, C3′-endo, g^-, ω,ω' (320,330°), $g'g'$, gg, C3′-endo, anti, and a more loosely base-stacked loop structure, II, with anti, C3′-endo, g^-, ω,ω' (80°,50°), $g'g'$, gg, C3′-endo, anti orientations. Dimerization produces a number of nucleotidyl conformational changes including a shift in ribose equilibrium C2′-endo (S) ⇄ C3′-endo (N) in favor of C3′-endo in both Ap- and -pA (60:40 vs. 35:65 in monomers), a change in glycosidic torsion angle χ_{CN} toward 0°, and a greater locking-in of rotamers along bonds involved in the phosphodiester backbone. Moreover, there is clear evidence that the transitions from $S \rightarrow N$ forms and $\chi_{CN} \rightarrow 0°$ are directly related to base stacking in ApA. Finally, ApA exists in solution as an equilibrium between I, II and an unstacked form(s) with as yet undetermined conformational features. Since C4′–C5′, C5′–O5′, and C3′–O3′ bonds possess exceptional conformational stabilities, it is proposed that destacking occurs primarily by rotation about P–O5′ and/or O3′–P. Predominant factors influencing the overall ApA conformation are thus base–base interaction and flexibility about P–O5′ and O3′–P, with change of ribose conformation occurring in consequence of an alteration of χ_{CN}, the latter in turn being governed by the need for maximum π overlap of stacked adenine rings.

Ribodinucleoside monophosphates are the simplest repeating chemical and structural constituent units of polyribonucleotides, sRNA, mRNA. Accordingly, they are excellent models for evaluating conformational properties relevant to RNA structures (Ts'o, 1974). To date, the most comprehensive structural data have been obtained from x-ray crystallographic measurements (Sussman et al., 1972; Kim et al., 1973; Rosenberg et al., 1973; Stellman et al., 1973). Rather less definitive information is available from solution studies where interest has centered primarily on base–base orientation with less attention directed toward conformational properties of ribose rings and the phosphodiester backbone. In view of the success achieved by NMR spectroscopy in defining intermolecular interactions (Schweizer et al., 1965; Broom et al., 1967) and overall conformations for monoribonucleotides (Danyluk and Hruska, 1968; Schweizer et al., 1968; Schirmer et al., 1972; Hruska et al., 1970, 1973; Sarma and Mynott, 1973; Altona and Sundaralingam, 1973; Davies and Danyluk, 1974, 1975), it seems natural to extend this approach to conformational studies of dinucleoside monophosphates in solution.

A number of NMR investigations have already been reported in this area, among the most extensive being those of Ts'o and co-workers (Ts'o et al., 1969) who measured base proton and anomeric H1′ shifts and H1′H2′ spin couplings for a large number of mixed dinucleoside monophosphates at various solution conditions. Most of the earlier studies (Ts'o et al., 1969; Chan and Nelson, 1969; Hruska and Danyluk, 1968a,b) attempted to determine base–base and base–ribose orientations, typically by comparing dimerization shifts (or temperature effects thereon) with those predicted for various possible model structures. For example, selective upfield shifts for H2, H8, and H1′ signals of ApA[1] appeared to fit a stacked anti structure with a right helical axis rather than other possible structural models (Ts'o et al., 1969; Chan and Nelson, 1969). NMR has also been used to study dynamical properties of stacked bases and mechanisms for destacking. Thus, observation of H1′H2′ coupling changes established that thermally induced base destacking of ApA and other adenylate dimers is accompanied by an alteration in ribose ring conformation (Hruska and Danyluk, 1968b). More recently Kan et al. (1973), in an ingenious series of measurements, utilized stacking shift changes for selected dinucleoside monophosphate derivatives in combination with other physicochemical measurements to show that base destacking occurs by an "oscillation–rotation" mechanism (Davis and Tinoco, 1968) rather than a simple, two-step stacked ⇌ unstacked process.

Although the earlier investigations have given some insights into dimer structures, a large amount of spectroscopic information particularly useful for fixing ribose ring and phosphodiester backbone conformations has not been avail-

† From the Division of Biological and Medical Research, Argonne National Laboratory, Argonne, Illinois 60439. *Received August 25, 1975.* This work was supported by the U.S. Energy Research and Development Administration. This is paper III of a series on NMR studies of nucleic acids in solution.

‡ Now at the Department of Chemistry, Federal City College, Washington, D.C. 20005.

[1] Abbreviations: ApA, adenylyl-3′→5′-adenosine; TSP, 3-trimethylsilylpropionate-2,3,3,3-d_4 sodium salt.

able because of difficulties in making direct, unequivocal assignments for protons of these groups. The problem is especially acute for homodimers, i.e., XpX, where base signal assignments require recourse to structural models, the dimerization shifts in turn being used to confirm the structure. To circumvent this difficulty, we have developed a selective labeling (^2H) approach in which one of the nucleotidyl units of a dimer is replaced by its fully deuterated counterpart (Kondo and Danyluk, 1972). Assignment of proton signals for the other nucleotide follows directly. The method has been applied to a number of dinucleoside monophosphates (Kondo, Leung, and Danyluk, 1973) including a preliminary assignment of the ApA spectrum reported elsewhere (Kondo and Danyluk, 1972, 1974). The assignment for the latter is in essential agreement with very recent spectral simulation results (Lee et al., 1975).

We now report a comprehensive proton NMR study of ApA undertaken with the objectives of obtaining a complete set of accurate chemical shifts and couplings, and utilizing these in turn to define the dynamically averaged conformation in aqueous solution. The results yield a detailed composite conformational model for ApA, and reveal a number of interesting conformational similarities and differences with other dimers in the crystalline state and monomers in solution.

Experimental Section

Materials. ApA (Na salt), adenosine, 3′-AMP and 5′-AMP (Na salts) were all purchased from Sigma Chemical and were used without further purification. The ApA showed no traces of impurities or decomposition products on paper chromatography. Dicyclohexylcarbodiimide used in synthesis of the labeled dinucleotides was purchased from Schwarz/Mann. D_2O (99.8%) was obtained from the USAEC and 100% D_2O used for preparation of final solutions was purchased from Diaprep, and Stohler Isotope Chemicals. 3-Trimethylsilylpropionate-*2,3,3,3-d*$_4$ sodium salt (TSP) was purchased from Merck, Sharp and Dohme.

Synthesis of Labeled ApA. 2,1′,2′,3′,4′,5′,5′-Heptadeuterioadenylyl-(3′-5′)-adenosine (*ApA) and adenylyl-(3′-5′)-2,1′,2′,3′,4′,5′,5′-heptadeuterioadenosine, (Ap*A) were synthesized by the procedure of Lohrmann and Khorana (1964). In each instance, the asterisk superscript denotes a fully deuterated (except H8) nucleotidyl group. Full details for the *ApA synthesis have been presented elsewhere (Kondo et al., 1973). Similar steps were followed for the Ap*A synthesis except that the starting materials for the condensation were pyridinium *N,O*$^{2′}$,*O*$^{5′}$-tribenzoyladenosine 3′-phosphate and fully deuterated 2′,3′-isopropylideneadenosine. Both the *ApA and Ap*A were purified by paper and DEAE-cellulose chromatography and yielded in each instance a final product chromatographically identical with a standard ApA sample.

Preparation of Solutions. In order to reduce the residual HDO peak to a manageable intensity, a weighed quantity of nucleotide and reference TSP was lyophilized from 99.8% D_2O solution (~50 ml) four to five times and the final lyophilized sample dissolved in an appropriate amount of 100% D_2O under a dry, inert (N_2) atmosphere.

Concentrations of the lyophilized dimer and monomer solutions were adjusted to a molarity (0.038 M) sufficient to give a reasonable signal-to-noise ratio, yet low enough so that intermolecular effects are minimal. All of the solutions were unbuffered to eliminate possible buffer counterion effects; measured pD values were in the range ~6.7–7.0. The TSP was kept at concentrations ~1–2 × 10^{-3} M, where intermolecular effects are negligible.

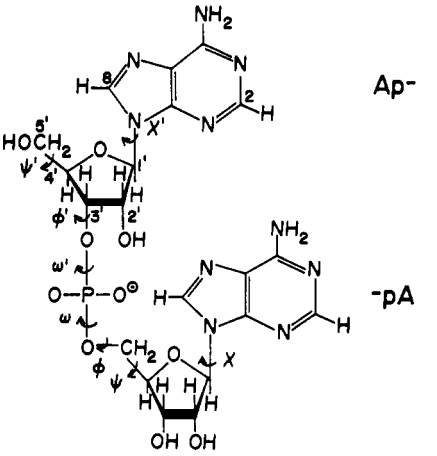

FIGURE 1. Chemical structure, torsion angle notation, and numbering scheme for adenylyl-3′→5′-adenosine; Ap- designates a nucleotidyl unit with the phosphate at C3′, while -pA designates a unit with the phosphate at C5′.

Measurement of Spectra. A Varian 220-MHz spectrometer, equipped with a variable temperature controller and Varian 620i computer, was used for measurement of all proton spectra (except for the FT spectrum of Ap*A). Spectra were recorded at 18 ± 2 °C, and spectral calibrations were made by the audio side-band method, employing a Hewlett-Packard 4204A oscillator linked with a Hewlett-Packard 5245 L frequency counter. Signal positions were measured relative to internal TSP and are accurate to ±0.1 Hz. Phosphorus decoupling experiments were carried out with a Schomandl ND 100 M frequency synthesizer connected to the probe through an ENI Model 310 rf amplifier and adjusted to the appropriate decoupling frequency (~89 MHz). A slight heating of the solution occurred in decoupling the relatively large ^{31}P–H(3′) coupling, and the temperature controller was used to maintain the tube contents at 18 °C.

Initial spectral simulations were made with a Varian 6-spin NMR simulation program on a 620i (8K) computer. The resultant parameters were then further refined using NMREN and NMRIT iterative programs. The NMRIT plot subroutine was modified to permit a composite plot of Ap- and -pA data, yielding a complete calculated ApA spectrum.

Results

1. Assignment of Signals. Because of the similarity in chemical structure of the nucleotides in ApA (Figure 1), an unambiguous assignment of signals to specific nucleotides is impossible from inspection of the 220-MHz spectrum alone (Figure 2A). Tentative assignments of base H(2), H(8), and ribose H(1′) signals deduced from considerations of deuterium exchange (H8 exchanges more rapidly than H2), adenine ring anisotropy effects in "stacked" ApA dimers, and paramagnetic ion induced signal broadening, were reported some time ago (Hruska and Danyluk, 1968a,b; Ts'o et al., 1969; Chan and Nelson, 1969), but these approaches did not yield a complete identification of ribose ring and ribose phosphate backbone protons. Furthermore, there is always a question regarding the validity of assumptions made in arriving at such "indirect" assignments. Spectral simulation (Lee et al., 1975) may be used to arrive at assignments

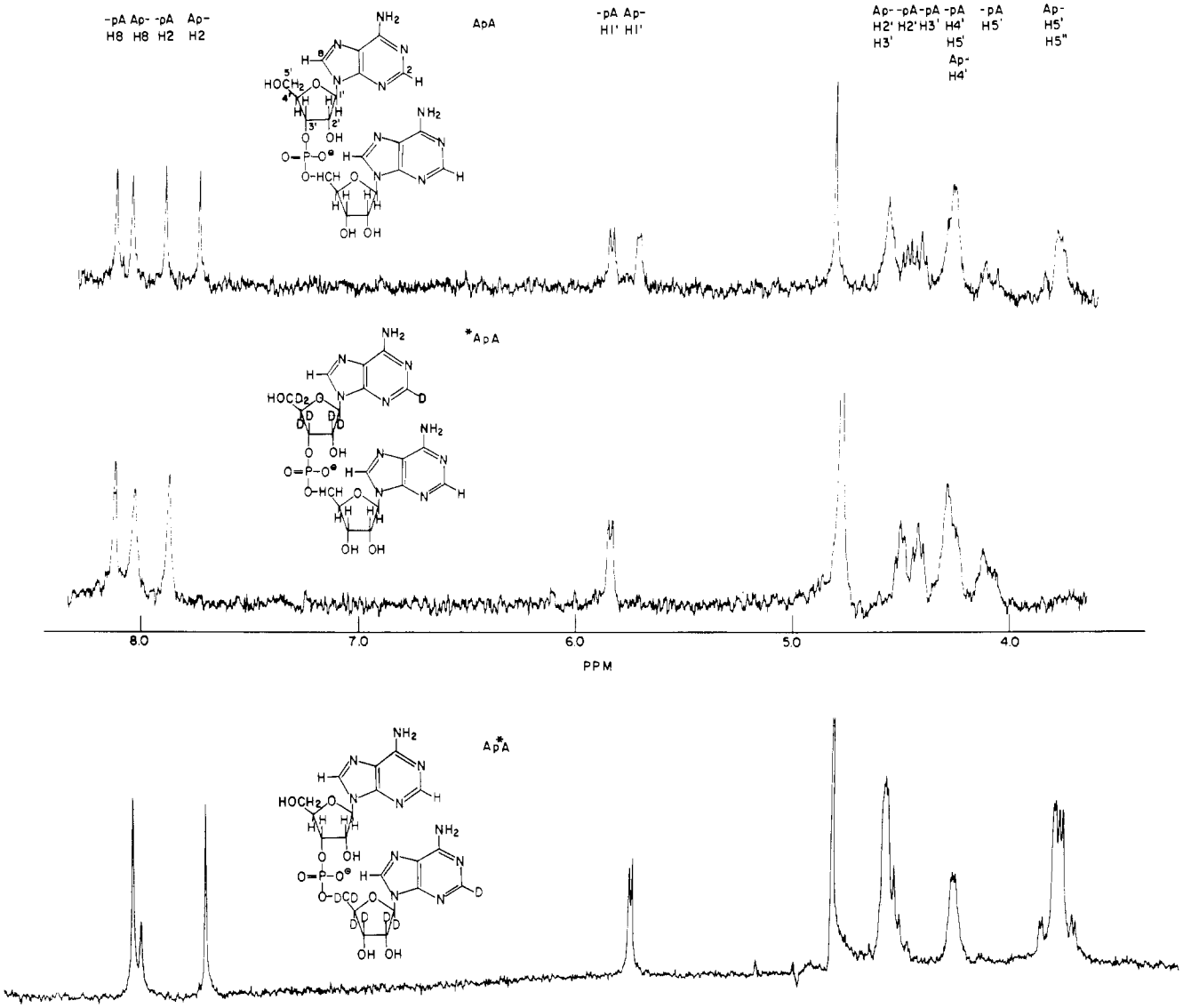

FIGURE 2. The 220-MHz proton spectra for ApA (upper spectrum), *ApA (middle spectrum), and $A\overset{*}{p}A$ (lower spectrum). Spectra were recorded for ~0.036 M concentrations in D_2O at pD ~6.5, and 18 °C. The spectra for ApA and *ApA are single scan in the CW spectrometer mode, while $A\overset{*}{p}A$ was measured in the FT mode (100 scans).

but this method has pitfalls when applied to homo-oligonucleotides (Kondo et al., 1975). Use of labeled derivatives eliminates the above problems. Thus comparison of the 220-MHz proton spectra for *ApA and ApA under similar concentration, 0.038 M, and solvent conditions (18 °C, pD ~6.9) permits a simple, direct assignment of signals (except those for H8 protons) to individual Ap- and -pA nucleotides (Figures 2A and B). Although only one labeled dimer, i.e., *ApA, was needed for an assignment, preparation of $A\overset{*}{p}A$ proved necessary for determination of all ribose proton coupling constants in Ap-. The $A\overset{*}{p}A$ spectrum shown in Figure 2C provides a confirmation of the assignment arrived at from A and B.

Back-exchange of protons for D8 during isolation and synthesis steps of *ApA and $A\overset{*}{p}A$ prevented an assignment of H8 signals but an alternative approach involving synthesis of 8-deuterio-adenylyl-(3′-5′)-adenosine from 8-deuterio-$N,O^{2'},O^{5'}$-tribenzoyladenosine 3′-phosphate and $N,N,O^{2'},O^{3'}$-tetrabenzoyladenosine yielded a compound whose proton spectrum showed a 50% decrease of signal intensity for the H8 signal at higher field, thereby identifying H8 of Ap-.

A further assignment of multiplets to specific 2′,3′,4′,5′5″ protons within each nucleotide was arrived at by inspection of multiplet patterns supplemented by appropriate ^1H-^1H and ^1H-^{31}P decoupling experiments. For example, for the -pA nucleotide, the two pseudo triplets at 4.57 and 4.51 ppm are clearly due to H2′ and H3′. Irradiation of the H1′ (-pA) doublet at 5.95 ppm produced a collapse of the pseudo triplet at 4.57 ppm, permitting assignment of this multiplet to H2′ (-pA). Specific assignment of the two C5′ protons in -pA is somewhat more difficult since ^1H-^1H or ^1H-^{31}P decoupling results alone are not sufficient for the purpose though the latter simplified the -pA C5′ proton multiplet pattern at 4.18 ppm from a doublet of triplets to a doublet of doublets thereby allowing extraction of all the relevant coupling constants to this proton. Remin and Shugar (1972) have shown, however, that for a wide variety of nucleosides and nucleotides the C5′ proton signal at lower field is due to the proton located trans to C3′ in the gauche–gauche rotamer (C4′-C5′). Analogous considerations of shifts, and $J_{4'5'(5'')}$, $J_{^{31}P5'(5'')}$ values for various rotamer possibilities (cf. Discussion), show that the Remin-Shugar assignment also holds for C5′ protons of -pA.

Table I: Final Iterated NMR Parameters for Protons of ApA in D_2O[a] at 18°C.

Proton	Chemical Shifts (ppm)	
	Ap–	–pA
1′	5.831	5.949
2′	4.673	4.567
3′	4.664	4.512
4′	4.359	4.375
5′	3.900	4.379
5″	3.841	4.184
2	7.881	8.040
8	8.175	8.233
^{31}P	89,065,302[b]	89,065,302[b]

[a] Shifts are relative to internal TSP and are accurate to ±0.005 ppm. [b] Given in frequency units.

Table II: Spin Coupling Constants for ApA in D_2O at 18 °C.

Coupling Constants[a] (Hz)	Nucleotidyl Unit	
	Ap–	–pA
1′2′	3.6	4.0
2′3′	5.2	5.3
3′4′	5.5 ± 0.2	5.8
3′5′	<0.2	<0.2
3′5″	<0.2	<0.2
4′5′	2.5	2.8 ± 0.3
4′5″	3.5	3.7
5′5″	−13.2	−12.0
^{31}P2′	<0.2	<0.2
^{31}P3′	7.6 ± 0.4	<0.2
^{31}P4′	<0.5	1.4 ± 0.4
^{31}P5′	0	3.0 ± 0.3
^{31}P5″	0	3.3

[a] Coupling constants are accurate to ±0.1 Hz except as noted.

Hence H5′ is identified with the multiplet at lower field, 4.38 ppm, and denotes a proton trans to C3′ in a *g*–*g* rotamer.

Similar steps were followed for specific assignments of Ap- signals, except that double irradiation at H1′, 5.83 ppm, and H4′, 4.36 ppm, does not sort out the closely coupled H2′ and H3′ signals. A final assignment of the latter was therefore made from comparison of calculated and observed spectra run at expanded sweep widths (50–100 Hz). The two C5′ protons again conformed to the behavior noted by Remin and Shugar (1972), and the signal at lower field is accordingly assigned to H5′ trans to C3′ (*gg* rotamer).

The final complete assignment of all the signals for ApA is shown in the upper part of Figure 2.

2. Determination of NMR Parameters (δ, J). Since there are no internucleotide spin couplings, the ribose phosphate regions of spectra for Ap- and -pA were analyzed independently. Considering -pA first, an approximate set of δ and J values was extracted for 1′, 2′, 3′, and 4′ protons from inspection of relevent multiplet patterns and assuming first-order splittings. These served as input parameters for spectral simulations (620i) and comparison with observed spectra recorded at 50 and 100 Hz widths led in turn to an improved set of δ and J's. Simulations were next made for the portion of the spectrum containing -pA 3′, 4′, 5′, 5″ protons, with the latter two coupled to ^{31}P. Because initial values of $J_{4'5'}$, $J_{^{31}P5'}$ and $\delta_{4'}$, $\delta_{5'}$ could not be picked out directly from the -pA spectrum at 20 °C, estimates were made at temperatures where overlap is less severe. Finally, the entire seven-spin -pA spectrum was calculated iteratively to give a complete refined set of coupling constants and chemical shifts. The iterated coupling constants differed by varying amounts (10–20%) from "first-order" values with adjustments being most noticeable for $J_{1'2'}$, i.e., 4.0 ± 0.1 Hz (final) vs. 3.7 Hz (doublet separation). The latter difference arises from residual virtual coupling interactions in the 1′2′3′ ABX-type spin system at 220 MHz. This influence will be magnified considerably at lower resonance frequencies where $(\delta_2 - \delta_3) \rightarrow 0$ and earlier $J_{1'2'}$ values, measured from H1′ doublet splittings alone at 60 and 100 MHz, are in error by substantial amounts. A check of $J_{4'5'}$, $J_{4'5''}$, $J_{5'5''}$, $J_{^{31}P5''}$ and $\delta_{4'}$, $\delta_{5''}$, $\delta_{5''}$ values was made by comparing a calculated 4′, 5′, 5″ multiplet pattern in the absence of ^{31}P coupling with an observed ^{31}P decoupled spectrum; excellent agreement was noted between the two.

Parameters for 1′, 2′, 3′ protons of Ap- were somewhat more difficult to determine because of overlap of H2′ and H3′ multiplets. Nevertheless, estimates of $J_{2'3'}$, $J_{3'4'}$, and $J_{^{31}P3'}$ couplings for simulation were achieved as follows. A value of $J_{2'3'} = 5.0$ Hz was estimated on the basis that $J_{2'3'}$ is nearly constant at 5.0 ± 0.2 Hz in virtually all of the 3′- and 5′-ribonucleotides. No change in $J_{2'3'}$ would be expected in going to dinucleotides. A value of $J_{3'4'} = 5.7$ Hz was obtained from inspection of the H4′ multiplet pattern in Ap*A, while $J_{^{31}P3'} \sim 7.6 \pm 0.4$ Hz was estimated from a comparison of normal and ^{31}P decoupled H2′, H3′ multiplet patterns. The remaining couplings $J_{1'2'}$, $J_{4'5'}$, $J_{4'5''}$, and $J_{5'5''}$ were derived from splitting patterns of respective protons; of some note is the well-resolved AB (of ABX) pattern for H5′, H5″ as distinct from the much more collapsed spectrum for 3′-AMP. As with -pA, a sizeable virtual coupling effect occurs for the H1′ doublet of Ap- and accounts for the difference between the present full analysis $J_{1'2'}$ value of 3.6 ± 0.1 Hz and earlier values of ~3.0 Hz measured from doublet splittings.

A summary of final best-fit δ and J values for ApA is given in Tables I and II, while the agreement between observed and calculated spectra is shown in Figure 3. The coupling constants and chemical shifts are accurate to ±0.1 Hz and ±0.005 ppm except in those cases where signal overlap introduced a somewhat greater uncertainty. As noted above, the $J_{1'2'}$ results differ from earlier values because of virtual coupling effects. Discrepancies also exist between ^{31}P couplings determined in this work and an earlier set of couplings measured from the phosphorus spectrum of ApA (Tsuboi et al., 1969). Tsuboi and co-workers (1969) ascribe $J_{^{31}PH}$ couplings of 3.4 and 6.5 Hz to unequal P–O–C5′–H5′(5″) interactions and a coupling of 8.1 Hz to P–O–C(3′)–H3′. No satisfactory fit of the observed ApA proton spectrum could be obtained for either the Ap- (H3′) or -pA (H5′, H5″) regions using all combinations of Tsuboi and co-workers coupling data raising some questions about the earlier J values. A considerable error could arise, however, from difficulties in estimating splittings from a complex phosphorus multiplet pattern with low signal-to-noise (see Figure 1 of Tsuboi et al., 1969) and possible effects of pD on the ribose phosphate backbone; the present measurements were made at pD ~6.5, while the phosphorus study was carried out at pD 9.2. Much better agreement is seen between the present parameters and values reported by Lee et al. (1975).

3. Comparison of ApA Monoribonucleotide Parameters.

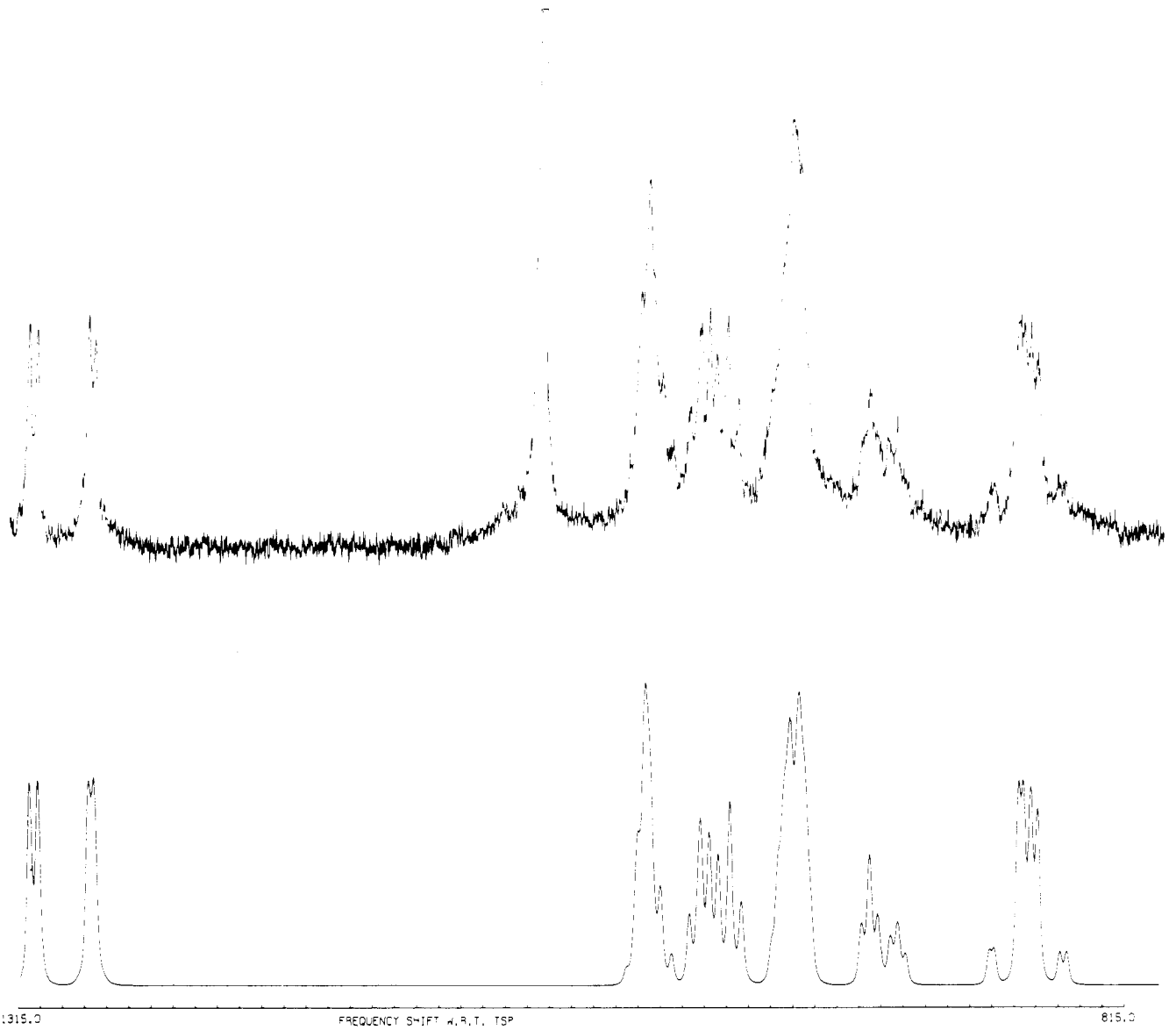

FIGURE 3. Observed (upper) and simulated (lower) spectra for ApA at 220 MHz. Solution concentration and conditions are the same as for Figure 2.

In order to assess dimerization effects on a consistent basis, δ and J values were determined for 3′-AMP, 5′-AMP, and ApA under conditions where intermolecular aggregation effects are absent and the degree of phosphate group ionization is identical for all nucleotides. Both factors are likely to have a bearing upon chemical shifts of base and ribose protons. It is known, for example, that H8 protons of 5′-AMP and other purine 5′-nucleotides show a sizeable deshielding with decreasing pH in the range 5–9, where the phosphate group undergoes a change in ionization state from −2 to −1 (Danyluk and Hruska, 1968; Schweizer et al., 1968). To adjust for this variable, spectral parameters were determined for 3′-AMP and 5′-AMP in solutions at pD 5.0, where secondary phosphate ionization is minimal. For 5′-AMP, a change in ionization state from −2 to −1 produced an upfield shift of 20 Hz for H8, and smaller upfield shifts ranging from +2 to +7 for 1′, 2′, and 3′ protons. More surprisingly, a large deshielding of −15 Hz occurred for both 5′ protons, while smaller deshieldings of −2 and −4 Hz resulted for H2 and H4′. An H5′(5″) deshielding is unexpected from changes of electronegativity alone. A possible explanation of this result can be given in terms of χ_{CN} differences and changes in rotamer populations about C(4′)-C(5′) and C(5′)-O(5′) bonds in 5′-AMP^{-1} and 5′-AMP^{-2} but further work is necessary to confirm this point (Danyluk and Ezra, 1975). Deshieldings also occur for H2′ (−6 Hz), H3′ (−12 Hz) and H4′ (−7 Hz) of 3′-AMP in going from −2 to −1 states. Only minor changes (−1 to +5 Hz) were observed for remaining ribose ring and base protons. Again, the observed results are opposite to the expected behavior and must be accounted for by rotamer changes about C(3′)-O(3′).

Appreciable concentration dependencies are known for H2, H8, and H1′ of purine nucleotides and are associated with intermolecular stacking interactions between purine rings (Evans and Sarma, 1974b, and references therein). An adjustment for these aggregation effects was made by determining parameters for each nucleotide at a number of concentrations and then extrapolating to infinite dilution values. For 5′-AMP and 3′-AMP, the largest adjustments were noted for H2 and H8 (−25, −8 Hz (5′-AMP) and −17, −9 Hz (3′-AMP); 0.04 M to infinite dilution); ribose

protons showed much smaller changes ranging from −6 (H1′) to +5 Hz (H4′, 3′-AMP). Adjustments for ApA parameters were significantly larger reflecting a greater tendency for self-aggregation of dimers compared with monomers over the same concentration range, 0.04 M to infinite dilution. For example, shift changes amounted to −33, −25, and −17 Hz for H2, H8, and H1′ of Ap- (0.04 M → 0); shift changes of similar magnitude occur for corresponding protons of -pA. One anomalous feature of the dimer concentration dependence was an *upfield* shift of +13 Hz for -pA H2′.

The infinite dilution parameters were used to calculate dimerization effects for each nucleotidyl unit as summarized in Table III. In line with earlier work, both sets of base protons show upfield shifts in the dimer with the trend in Ap-, $\Delta\delta$H2 > $\Delta\delta$H8 being opposite to that in -pA, $\Delta\delta$H8 > $\Delta\delta$H2, and also $\Delta\delta$H2(Ap-) > $\Delta\delta$H2(-pA). This behavior arises from intramolecular base stacking effects and information about base orientations can be derived from the relative shift changes (cf. following section). All of the ribose protons of Ap- are shifted upfield relative to 3′-AMP[−1] by substantial amounts ranging from 43 Hz for H1′ to 17 Hz for H3′. A different behavior is seen for -pA where H1′ and H2′, particularly, show upfield shifts while H3′ and H4′ vary only slightly from the monomer; also the upfield trend $\Delta\delta$H1′ > $\Delta\delta$H2′ in Ap- is reversed in -pA. Unusual and interesting shift changes occur for both sets of C5′ protons, the set for Ap- exhibiting an upfield shift while that for -pA a *downfield* shift with H5′ (-pA) showing a striking deshielding of −56 Hz. Again, the changes in chemical shifts for ribose and exocyclic protons can be understood in terms of preferred conformational effects (Discussion).

Considering coupling constants, major variations occur for $J_{1'2'}$ and $J_{3'4'}$ in both nucleotides upon dimerization; moreover, the decrease of $J_{1'2'}$ is mirrored by a corresponding increase of $J_{3'4'}$; $J_{2'3'}$ is effectively unchanged. Previous work (Hruska and Danyluk, 1968b; Ts'o et al., 1969; Chan and Nelson, 1969) reported $J_{1'2'}$ (ApA) < $J_{1'2'}$ (monomer), but the magnitude of the change was obscured by virtual coupling effects on $J_{1'2'}$ (ApA). Ts'o et al. (1969) also expressed reservations that $J_{1'2'}$ changes reflected alterations of ribose conformations; this objection is clearly refuted by the present results showing an almost exact match between magnitudes of $J_{1'2'}$ and $J_{3'4'}$ changes as would arise from a ribose conformational change (cf. Discussion). Small, but detectable monomer-dimer differences also are observed in proton couplings across the C4′-C5′ bond and for $J_{^{31}PH5''}$ as might be expected for changes in conformational properties along these bonds.

Table III: Effects of Dimer Formation on NMR Parameters[a] of ApA.

	A. Chemical Shifts $\Delta\delta$(monomer−dimer)[b] (ppm) for ApA			B. Coupling Constants ΔJ(monomer−dimer) (Hz)[c]	
Proton	Ap- (3′)	-pA (5′)	Proton	Ap- (3′)	-pA (5′)
2	0.236	0.068	1′2′	2.7	1.8
8	0.073	0.195	2′3′	NC	−0.2
1′	0.195	0.118	3′4′	−2.7	−2.1
2′	0.118	0.268	3′5′	NC	NC
3′	0.077	−0.005	3′5″	NC	NC
4′	0.114	0.018	4′5′	0.5	0.2
5′	0.064	−0.255	4′5″	−0.5	−1.2
5″	0.095	−0.068	5′5″	−0.3	0.7
			2′P	NC	NC
			3′P	−0.3	NC
			4′P	NC	NC
			5′P	NC	NC
			5″P	NC	−0.8

[a] Both monomer and dimer parameters are adjusted to infinite dilution values; mononucleotide parameters were also determined for a PO_4^- ionization state. For comparative purposes, nucleotide Ap- is considered to be derived from 3′-AMP and -pA from 5′-AMP. [b] Negative sign denotes downfield shift in dimer. [c] Negative sign denotes an increase in the dimer; NC = no change.

Discussion

A dinucleoside monophosphate has conformational flexibility about eight bonds (Figure 1), along with the existence of conformational equilibria in both ribose rings. In order to arrive at the dynamically averaged structure for ApA in solution, conformational preferences must be established for all eight torsion angles and for each ribose ring. For four of these, ϕ, ψ, ψ', ϕ', the necessary information is available from ^{1}H-^{1}H and ^{1}H-^{31}P couplings, while chemical shift data give an insight into orientations about the remaining four, χ, χ', ω, ω'. Similarly an analysis of ^{1}H-^{1}H ring couplings permits conformational deductions for ribose rings. By combining all the relevant results, a composite model may be constructed for ApA as outlined in the following.

D-Ribose Ring Conformations. Precise calculations of all pseudorotational parameters (pseudorotational angle, P; degree of pucker, τ_m), and ring conformer populations for the equilibrium between type N and type S conformers, i.e., $N \rightleftharpoons S$, from measured $J_{1'2'}$, $J_{2'3'}$, and $J_{3'4'}$ values can be made by the pseudorotational method (Altona and Sundaralingam, 1972, 1973). The AS (Altona-Sundaralingam) method has been utilized in conformational analyses for various nucleosides and nucleotides (Altona and Sundaralingam, 1973), and in systematic studies of 2′-, 3′-, and 5′-ribonucleotides and 5′-deoxyribomononucleotides (Davies and Danyluk, 1974, 1975).

Recent criticisms (Evans and Sarma, 1974a) raise cogent questions regarding the validity of using a generalized Karplus equation, the influence of intrinsic errors in coupling constant magnitudes, and the assumption of constancy of $J_{2'3'}$ and $J_{1'2'} + J_{3'4'}$. Evans and Sarma's example of 5′-AMP and our own analyses of ribo- and deoxyribonucleotides (Davies and Danyluk, 1974, 1975) show that slight changes in any of these factors can have a significant impact upon calculated values of P, τ, and ring conformer populations. In light of this, Evans and Sarma suggest that semiquantitative methods, which consider the D-ribose ring as a rapidly equilibrating mixture between classical C3′-endo (^3E, P = 18°) and C2′-endo (^2E, P = 162°) forms, viz., $^3E \rightleftharpoons {}^2E$, though not as conceptually sophisticated as the AS approach, nevertheless permit a meaningful evaluation of conformer populations from ring coupling data.

With these considerations in mind, and noting that $J_{2'3'}$ and $J_{1'2'} + J_{3'4'}$ are nearly constant in ApA, 5′-AMP, and 3′-AMP, we have employed the full AS analysis, in conjunction with calculated curves similar to those of Figure 6 (Davies and Danyluk, 1974) to derive sets of pseudorotational parameters and conformer populations listed in Table IV. Constants for the Karplus expression, $J(H,H) = A\cos^2\theta + B\cos\theta$, were obtained by procedures described previously (Davies and Danyluk, 1974) and yielded values of A = 10.0, B = −0.9, very close to those for 5′- and 3′-ribomononucleotides.

Table IV: Ribose Ring Conformational Properties Calculated from NMR Parameters.

Nucleotide	P_N	P_S	N_{τ_m}	S_{τ_m}	Mole Fraction N	K_{eq}[a]	K_{eq} (S)[b]
ApA							
Ap–	18	164	35	37	0.62	1.63	1.61
–pA	24	168	36	37	0.59	1.44	1.45
3′-AMP	14	169	35	38	0.34	0.51	0.51
5′-AMP	17	165	37	40	0.38	0.62	0.61

[a] K_{eq} for $S \rightleftharpoons N$. [b] $K_{eq}(S)$ by simple approach (Davies and Danyluk, 1974).

Table V: Rotamer Populations about Exocyclic Conformational Bonds.

	Populations (%)								
	C4′–C5′[a]			C5′–O5′[b]			C3′–O3′[c]		
Nucleotide	gg	tg	gt	g′g′	t′g′	g′t′	g+	g−	t
ApA									
Ap–	85	2	13					~40°	
–pA	75	8	17	86	6	8			
3′-AMP	74	18	8					~30°	
5′-AMP	76	12	12	74	13	13			

[a, b] Equations used for rotamer calculations (rotamer designations are as in Davies and Danyluk, 1974, 1975):

C4′–C5′[a] $gg = (13.8 - \Sigma(J_{4'5'} + J_{4'5''}))/9.7$ (1)

$tg = (J_{4'5'} - J_g)/9.7$ (2)

$gt = (J_{4'5''} - J_g)/9.7$ (3)

C5′–O5′[b] $g'g' = (22.6 - \Sigma(J_{5'P} + J_{5''P}))/19.0$ (4)

$t'g' = (J_{5'P} - J_g)/19.0$ (5)

$g't' = (J_{5''P} - J_g)/19.0$ (6)

[c] Populations could not be calculated about this bond but use of the appropriate empirical correlation (Davies and Danyluk, 1975) permits calculation of appropriate vicinal angles (cf. text).

The calculated pseudorotational angles and degree of pucker are largely of semiquantitative interest given their susceptibility to computational errors. Nevertheless, it is worth noting that the present P_N values of 18 and 24°, and P_S of 164–168° for Ap- and -pA nucleotides are concordant with N and S conformations that are nearly C3′-endo (^3E), P = 18° and C2′-endo (^2E), P = 162°, respectively. Also, the apparent differences in P_N from monomer values of 14–17° are outside the limits (±5°) expected from computational errors. If this is so, then the P_N values suggest that the ribose ring changes from an unsymmetrically twisted N form, i.e., C3′-endo, C2′-exo ($^3T_2$) in adenine mononucleotides to a more symmetric envelope conformation typified by ^3E. In contrast, dimerization produces no significant change for either P_S or τ values. Note, however, that τ_m values are relatively insensitive to ribose couplings (Figure 6, Davies and Danyluk, 1974).

Of perhaps greater quantitative interest are calculated conformer populations and equilibrium constants for the process $S \rightleftharpoons N$. These parameters are less subject to computational errors in the AS approach and can also be evaluated by a simpler, more direct, but somewhat less quantitative procedure employed in other studies (Evans and Sarma, 1974a,b; Davies and Danyluk, 1974; Hruska, 1973). In fact, comparison of K_{eq} values in Table IV shows excellent agreement between the two approaches. The results show a C3′-endo (N) dominance in both Ap- (62% N) and -pA (59% N), whereas the opposite holds for constituent monomers, i.e., 34 and 38% N respectively, at equivalent residue concentrations. A shift from S (C2′-endo) to N (C3′-endo) conformers clearly occurs upon dimerization as was suggested some time ago from $J_{1'2'}$ changes alone (Hruska and Danyluk, 1968b). In their more recent work, Altona and Sundaralingam (1973) calculated N conformer populations of 68% (Ap-) and 65% (-pA) from then existing $J_{1'2'}$ values. The uniformly higher N populations of the latter work reflect the use of an incomplete set of ribose ring couplings along with first-order $J_{1'2'}$ values. In comparing monomer and dimer data, it should be pointed out that the N conformer becomes progressively more favored as 5′-AMP (Evans and Sarma, 1974) and 3′-AMP (Kondo and Danyluk, 1975) concentrations increase with a cross-over at concentrations of ~1.5 to ~2.0 M. The switch from S to N correlates directly with increased stacking of adenine nucleotides at higher concentrations. Whether the ribose change reflects a direct intermolecular effect of an adjacent nucleotide or an indirect effect mediated via the glycosidic torsion angle remains to be established. According to Arnott (1972), an S conformation is less favored in helical polyribonucleotides because intramolecular contacts are more crowded in stacked C2′-endo forms (we are indebted to a reviewer for pointing out this reference). The relationship between ribose ring conformation and stacking is explored further in a following section.

Within the error range of our calculations, there does not appear to be any significant difference in N (C3′-endo) conformer populations in the two nucleotidyl residues (Table IV). There is, however, a somewhat greater population change in going from 3′-AMP to Ap-, ΔN = +0.28, then for the 5′-nucleotide, ΔN = +0.21, suggesting a somewhat lower barrier to conformer interconversions in the latter.

Although crystallographic parameters are not yet available for ApA, the dimer ribose conformations in solution agree with results of a recent x-ray diffraction study of $A^-pA^+p^-A^+$ (Suck et al., 1973) which show all three ribose rings in a C3′-endo envelope conformation with a somewhat greater pucker of Ap- vs. $-Ap^+-$ residues.

Ribose–Phosphate Backbone Conformation. For simplicity, the conformational properties of the backbone will be considered in terms of five bonding arrangements, C4′–C5′, C5′–O5′, C3′–O3′, O5′–P, and P–O3′.

C4′–C5′ (ψ,ψ'). Both nucleotidyl residues possess conformational flexibility about this bond. In line with extensive previous analyses for mononucleotides (Davies and Danyluk, 1974, 1975) and nucleosides (Hruska et al., 1973; Hruska et al., 1974), the conformational properties can be considered in terms of rapid rotational averaging among three classical staggered rotamers, *gg*, *tg*, and *gt*. A straightforward evaluation of *gg* rotamer populations can be made from the sum of $J_{4'5'}$ and $J_{4'5''}$, i.e., eq 1, Table V, whereas calculation of *gt* and *tg* populations requires specific assignment of H5′ and H5″. A tentative assignment for these protons in Ap- and -pA residues was given in a preceding section.

Since vicinal coupling data are not available for pure trans and gauche rotamers for bonding arrangements of types O–C–C–H, estimates of J_g = 2.0 Hz and J_t = 11.7 Hz were made from a modified Karplus relation (Blackburn et al., 1970). These values differ slightly from couplings used by others and are a source of uncertainty (5–10%) in all such rotamer calculations. Utilizing coupling

data from Table II and appropriate eq 1-3, Table V, mole fractions were calculated for *gg*, *tg*, and *gt* rotamers and are summarized in Table V. Within limitations of this analysis, there is an obvious marked preference for *gg* conformations about ψ (Ap-, C4′-C5′), 85 ± 7%, and ψ' (-pA, C4′-C5′), 75 ± 7%, followed in order by *gt* (13 and 17%) and *tg* (7, 8%) rotamers. The latter populations are subject to greater uncertainty due primarily to the impact of coupling error limits on the numerators of eq 2 and 3. However, there can be no question that *gg* conformations are overwhelmingly preferred over *gt* + *tg* in ApA at solution conditions encompassed in this work. When these preferences are further compared with rotamer populations for corresponding mononucleotides, there is found to be little, if any, change in *gg* population on dimer formation (Table V). Thus base-stacking and associated changes in glycosidic torsion angle (cf. following section) occurring on dimerization are not accompanied by a significant shift of *gt* + *tg* → *gg* (or vice versa) though there is a possibility that the ratio *gt*/*tg* shifts in favor of *gt* in both Ap- and -pA. The *gt*/*tg* rearrangement for the latter unit may be related to greater steric crowding in *tg*. An exceptional conformational integrity apparently exists about ψ and ψ' for nucleotides in solution; moreover the solution conformations about these bonds do not differ in any significant way from those for $Ap^-A^+p^-A^+$ in the crystalline state (Suck et al., 1973).

C5′-O5′ (ϕ). A conformational analysis utilizing coupling constant data can be made only for C5′-O5′ (ϕ) of -pA; exchange prevents detection of H-H couplings across this bond in Ap-. If a threefold rotational energy barrier with minima at 60, 180, and 300° is assumed for C5′-O5′, then observed ^{31}P-H couplings, in the limit of rapid rotation, are a weighted average of couplings in the three classical staggered rotamers (Table V). Rotamer populations are then given by equations derived elsewhere (Davies and Danyluk, 1974, Table VII). Since accurate values of J_t and J_g for pure rotamers are not as yet available, estimates of 20.8 and 1.8 Hz were obtained from a modified Karplus expression (Davies and Danyluk, 1974). A summary of rotamer populations calculated using ^{31}P-H coupling data is given in Table V. Again, it is found that the *g′g′* rotamer is markedly preferred (≃86%) over the combined *t′g′* and *g′t′* rotamers (≃14%). Further the percent *g′g′* appears to increase in going from monomer ≃75% to dimer and is only marginally affected by dimer concentration. Temperature increase and pH decrease, however, produce changes leading to a lesser *g′g′* rotamer purity (Kondo and Danyluk, 1975).

The preferred *g′g′* conformation about ϕ is very similar to conformations found for 5′-mononucleotides in the solid state where ϕ falls in a narrow range, about $\phi \simeq 180°$.

C3′-O3′ (ϕ′). A rotamer analysis about this bond in Ap- is less straightforward because only one vicinal coupling, i.e., $J_{^{31}P,3'}$ is available for population calculations. No analysis is possible for -pA because of exchange effects. An earlier summary (Davies and Danyluk, 1975) of conformational preferences about ϕ' showed that x-ray structure data and theoretical calculations were both in broad agreement that ϕ' lies in a range of 180-240° for virtually all nucleotides for which data are available. In this favored range, P-O3′ is approximately antiperiplanar to C3′-C4′ and approximately gauche (g^-), with respect to C3′-H3′, conformation 3, $\phi' = 180°$ (cf. Figure 6, Davies and Danyluk, 1975). No evidence was indicated for the other two classical staggered rotamers, i.e., gauche (g^+), P-O3′—C3′-H3′, ϕ' = 300° (conformation 2), and trans P-O3′—C3′-H3′, ϕ = 60° (conformation 1). In solution a consideration of $J_{^{31}P,H3'}$ coupling constants for a variety of 3′-ribonucleotides further indicated the magnitudes were best explained by either (i) a predominant approximately gauche g^-, conformation 3, (ii) an equilibrium mixture of equally populated g^- and g^+ conformations, or (iii) essentially free rotation among three equally populated g^+, g^-, t conformations. Comparison of ring proton shifts for 3′-ribo and deoxyribonucleotides ruled out the third possibility; such a rotamer equilibrium is even more unlikely in a dinucleotide because of steric hinderance. For the dimer the observed coupling of 7.6 Hz is best accommodated by possibilities (i) and/or (ii) with (i) being more in line with crystal data (Sundaralingam, 1969). An estimate of ~40° (ϕ' ~200) can be made for the dihedral angle H3′-C3′-O3′-P using the vicinal P-H correlation given earlier.

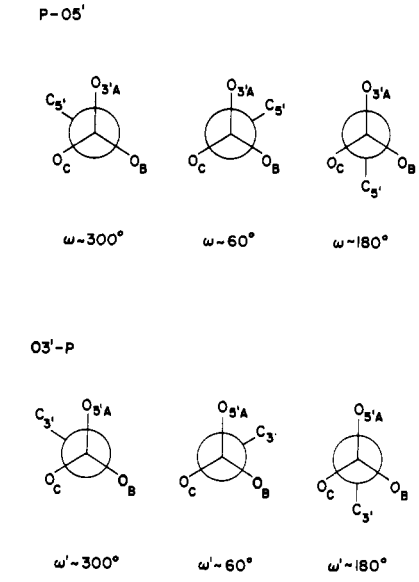

FIGURE 4. Classical staggered rotational isomers about P-O5′ and O3′-P bonds of a dinucleoside monophosphate. A symmetric threefold potential is assumed for each bond and torsion angle magnitudes follow Sundaralingam's convention (Sundaralingam, 1969).

O5′-P(ω) and P-O3′(ω′). A sorting out of conformations about these bonds cannot be made with coupling data since rotation does not alter any dihedral angles along ^{31}P, ^{13}C, or ^{1}H coupling paths. An insight can be gained, however, from chemical shift values for certain protons, but in order to utilize these, recourse is necessary to crystal structure data for polynucleotides and several dinucleotides.

The preferred range of ω found for phosphodiester linkages in the cystalline state is ~257-315° with most values centered about 290° (Figure 14 of Sundaralingam, 1969; and Sundaralingam, 1973). A smaller number of nucleotides cluster around ω ~60-80°, and dinucleotides for which crystal structure data are available show torsion angles of ω ~90 and ~290°. Both dihedral ranges lie close to expected values for two of the staggered rotamers about P-O5′ (Figure 4).

Three ω' ranges are found in the crystalline state (Sundaralingam, 1969) with most phosphodiesters having values around 270-300°; a smaller number have ω' of 60-80° and 160-180°. Dinucleotides generally have ω' values clustered at 64-81° and 280-290° with one UpA conformer having $\omega' = 163°$ (Sussman et al., 1972). These ranges

again encompass values near those for classical staggered rotamers about P-O3′ (Figure 4).

Attempts have also been made to predict ω and ω' angles for mono- and dinucleotides by theoretical conformational energy calculations. Classical potential energy (Broyde et al., 1974) and molecular orbital approaches (CNDO, Tewari et al., 1974; PCILO, Perahia et al., 1974) have been utilized and both show a global minimum in ω,ω' energy maps at values near 290,290°. CNDO calculations also show a second nearly isoenergetic minimum at 70,70°, while classical calculations reveal the second lowest energy region to be at ω,ω' values of 20 and 80°. Other local minima are predicted at somewhat higher energies but these do not conform to the majority of observed crystallographic conformations. Utilizing data from crystal structure determinations and results of theoretical calculations, Kim et al. (1973) proposed seven basic conformational units for dinucleoside monophosphates. Of these, two with ω,ω' angles of 280,290° (conformation I) and 80°,80° (conformation II) are favorable for stacking of bases, while the remaining five conformations do not allow base stacking. Conformations with $\omega,\omega' \sim$290,290° nucleate a right-hand helical structure and those with ω,ω' 80,80° a left-hand helix.[2]

No crystallographic data are available for ApA as yet but an insight into the phosphodiester conformation can be gained from the trinucleotide zwitterion structure for $Ap^-A^+p^-A^+$ reported recently by Suck and co-workers (1973). Two sets of ω,ω' angles were found, the Ap^-A^+ segment having ω,ω' of 279,281° and the $A^+p^-A^+$ segment, 92,76°. When combined with other conformational properties, i.e., anti orientations for all three adenylates, C3′-endo ribose rings and favored *gg*, *g′g′*, g^- backbone conformations, the net effect is a structure with two nucleotides, Ap^-A^+, stacked in a right-hand helix arrangement while the third nucleotide, $-p^-A^+$ is flipped with respect to $-p^-A^+p^-$- so that the adenylates are only loosely stacked with their ribose oxygens oriented in opposite directions. The helical and loop sections conform very closely to two of the basic conformations proposed by Kim et al. (1973).

These considerations lead us to assume that ω,ω' angles for ApA will not differ substantially from those for $Ap^-A^+p^-A^+$ and that any drastic conformational change in going from the crystalline state into solution is unlikely at least at room temperature or lower. Comparison of crystal and solution conformations shows this to be true for most mononucleotides and a similar situation is likely to hold for dimers.

For ApA the existence of a compact, conformationally "rigid" backbone structure with ω,ω' of 300,300° or $\sim$70,70° accounts well for the striking deshieldings of H5′ and H5″ of -pA. Qualitatively these deshieldings originate as follows: in a *gg*, *g′g′*, g^-, $\omega\omega'$ (300,300°) ribose phosphate bonding arrangement, the O5′-C5′ bond is located approximately gauche-gauche with respect to P-O3′ and P-O(C) bonds (Figure 4). In a locked conformation of this type, both H5′ and H5″ experience a greater deshielding effect from the negatively charged phosphate oxygens, i.e., O(C), then in the case for free rotation about P-O5′, e.g., 5′AMP. An estimate of $\Delta\delta$ (deshielding) is not feasible but examination of molecular models shows H5′ and H5″ to be roughly the same distance from O(C) suggesting similar deshielding magnitudes. A further consequence of the compact structure is enhanced exposure of H5′ to an additional deshielding influence of O2′ of Ap-; this is the likely origin of greater deshielding for H5′ than H5″. For a *gg*, *g′g′*, g^- $\omega\omega'$ (70,70°) arrangement, C5′-O5′ is approximately gauche,gauche to C3′-O3′, P-O(B) again exposing H5′,H5″ to greater deshielding by phosphate oxygens. In this instance, however, a further deshielding influence on H5′ from O2′ Ap- is impossible. No other conformational possibility about P-O3′, P-O5′, e.g., ω,ω' (180,180°) extended backbone, can account for -pA H5′,H5″ deshieldings while also being in accord with observed anomalous dimerization shifts for certain other protons, notably the large upfield shift of H2′ (-pA) and stacking shifts of H2 and H8 (cf. following discussion).

Glycosidic Torsion Angle χ_{CN} and Base-Base Orientation. The present adjusted (monomer-dimer) shift differences for base protons (Table III) are in line with earlier NMR (Chan and Nelson, 1969; Ts'o et al., 1969; Hruska and Danyluk, 1968b) and optical studies (Warshaw and Tinoco, 1965; Bush and Tinoco, 1967) showing the existence of stacked adenine rings in ApA at room temperature ($\sim$18 °C). In the stacked conformation, H2,H8 are primarily affected by the shielding regions of the adjacent adenine ring producing a net upfield shift whose magnitude depends upon interplanar distance, lateral interbase orientation, and glycosidic bond torsion angle (syn or anti). Consequently, the base protons are sensitive monitors of stacked structures and several attempts have been made to fix base orientations with shift data. For example, the observed order of increased shieldings, i.e., H2 (Ap-) > H2 (-pA) and H8 (-pA) > H8 (Ap-) (Chan and Nelson, 1969; Ts'o et al., 1969; Hruska and Danyluk, 1968a,b; also confirmed by the present adjusted shifts), and the much larger deshielding changes of H2 (Ap-) and H8 (-pA) with temperature increase (compared with H2 (-pA) and H8 (Ap-)) were qualitatively explained by a stacked anti dimer model having a right helical sense. Alternative stacked orientations, e.g., syn-syn, anti-syn, or syn-anti, were incompatible with observed trends (Chan and Nelson, 1969). However, the earlier dimer models were incomplete because no data existed to fix the connecting ribose phosphate backbone conformation. Inclusion of this conformational segment determined in the present study reveals that stacked anti (right helix) and loosely stacked anti loop orientations are readily accommodated within conformational constraints of the backbone.

A more quantitative description of base-base orientation can be made if reliable diamagnetic shielding anisotropies are known for the adenine ring, and if accurate measured base proton shifts for fully stacked and unstacked dimers are available. The latter information is not readily accessible since the observed shifts at 18 °C are actually weighted averages for a rapidly equilibrating mixture of stacked and unstacked forms, i.e., Stacked $\rightleftharpoons$ Unstacked and $\delta(H2) = N_S\delta_S + N_U\delta_U$, etc. Shifts for pure conformers, δ_S and δ_U can be extracted from δ vs. temperature curves if one assumes a simple $S \rightleftharpoons U$ equilibrium and adjusts for intermolecular aggregation effects at each temperature. The δ_S and δ_U values are not unambiguous, however, since analysis of the δ curve involves fitting a quadratic expression with δ_S, δ_U, and K_{eq} as variables. Nevertheless, a preliminary analysis of data over a 90°C temperature range yields δ_S-δ_U magnitudes of 0.29, 0.11 ppm for H2 and H8 of Ap- and 0.10, 0.27 ppm for H2 and H8 of -pA (Kondo and Dany-

[2] Strictly speaking a helix with ω,ω' of 80°,80° is sterically impossible (Kim et al., 1973) and energetically unfavorable (Yathindra and Sundaralingam, 1974) beyond the dinucleotide stage.

luk, 1975). The differences between these values and corresponding entries in Table III are accounted for by the presence of substantial amounts of unstacked ApA at 18 °C.

A comparison can now be made with stacking shifts obtained from calculated adenine isoshielding curves (Giessner-Prettre and Pullman, 1970). Starting with a stacked dimer model identical with Ap^-A^+ of the trimer, i.e., conformation I, ω,ω' 297,281° and 3.6 Å interplanar distance, stacking shift magnitudes of 1.1, 0, and 0.05, 0.12 ppm are estimated for H2 and H8 for Ap- and -pA, respectively. These values are clearly out of line with observed $\Delta\delta$'s but reasonable concordance is seen with relative trends (loc cit). Variation of the interplanar distance ±0.2 Å alters the absolute magnitudes somewhat but does not adjust for the divergence in relative magnitudes.

It is informative to explore what influence torsion angle changes have on stacked orientation in conformation I. Using Drieding models and imposing constraints of an approximately parallel base stacking and rotamer conformations fixed by coupling data, it can be shown that base alignments are critically dependent upon ω and ω'. Specifically, an increase of ω (290 → 360°) leads initially to a greater overlap ~310-320° followed by destacking (>360°), while a decrease leads to sterically unacceptable conformations. Rotation about ω' leads to greater overlap when ω' increased from 290 to 330°, and destacking when ω' decreases from 290 to 180°. The most favorable stack overlap and alignments occur in the region ω,ω', 320,330° for which predicted (stack) values are 0.32, 0.01 ppm and 0.04, 0.24 ppm for H2 and H8 of Ap- and -pA. These magnitudes are in better quantitative agreement with experimental $\Delta\delta$'s and relative trends are unchanged.

Following similar considerations, the most favorable geometry for stacking shifts in the loop conformation II occurs at ω,ω' of ~80,50°.[3] Estimated $\Delta\delta$ (stack) magnitudes are 0.10, 0.06 ppm and 0.10, 0.16 ppm for H2 and H8 of Ap- and -pA. For a mixture of stacked conformations I and II, the stacking shifts will be given by the weighted mean, i.e., $\delta_S(H2) = n_I\delta_S^I(H2) + n_{II}\delta_S^{II}(H2)$ and calculated values will lie between the values for I or II alone. The mean values are in closer approximation to measured $\Delta\delta$'s than is true for either conformation alone. This agreement is probably fortuitous, given the uncertainties of shielding calculations, but the analysis does suggest the existence of at least two stacked ApA conformations in solution.

Additional information on base-base orientations can be derived in principle from shift changes of ribose protons, but the situation is complicated by at least two base-related shielding effects, i.e., base stack, and changes of χ_{CN}. Considering the influence of base stacking alone in a type I conformation (ω,ω', 320,330°) upfield shifts relative to monomer would be expected in the order H2′ (Ap-) > H1′ (Ap-) > H3′ (Ap-) ~ H1′ (-pA); *no shielding changes* would occur for H2′ or H3′ of -pA since these protons are out of the shielding-deshielding range of the Ap- base. The predicted trend is not in good agreement with observed changes (Table III), the discrepancy being particularly noteworthy for H2′ (-pA) where a striking shielding increase of 0.27 ppm occurs relative to the monomer. This anomalous change cannot be attributed to any reasonable variation of conformation I. However, an alternative possibility, i.e., conformation II (80,50°), can produce upfield stacking shifts for 1′, 2′, and 3′ protons in both adenylyl units with the largest upfield shifts occurring for H2′ (of both Ap- and -pA) and less changes for H3′ and H1′. Qualitatively it would appear that the best correlation of observed and estimated trends is again obtained for a mixture of two stacked ApA conformations, but, of course, no estimate can be made of their relative proportions.

From isoshielding curves the magnitudes of stacking shifts are estimated as: Ap- (1′,2′,3′) 0.12, 0.08, ~0 ppm and -pA (1′,2′,3′) 0.01, 0, 0 ppm for conformation I (320,330°); and Ap- (1′,2′,3′) 0.06, 0.08, 0.03 ppm and -pA (1′,2′,3′) 0.04, 0.08, 0.02 ppm for conformation II (80,50°). Both conformations thus yield $\Delta\delta$ (stack) magnitudes substantially lower than measured shift changes. The spread can be narrowed somewhat by adjusting the conformation to smaller interbase distances (3.2-3.4 Å), but even under these conditions the estimated shifts are still ~0.1-0.2 ppm lower than observed. It is therefore questionable whether base stacking alone is responsible for increased ribose shieldings, and other potential nucleotidyl conformational changes were accordingly investigated. Of these, the most likely candidate is an alteration of the glycosidic torsion angle (χ).

From previous monomer studies (Davies and Danyluk, 1974), it is known that sizable downfield shifts occur for ribose protons of purine nucleotides relative to pyrimidines. These vary in order H2′ > H3′ > H1′ > H4′ and range in magnitude from 0.063 (H1′) to 0.359 ppm (H2′). A study of molecular models incorporating conformational properties deduced from crystal structure and NMR data further led to the conclusion that these shift differences arise from location of 1′, 2′, and 3′ protons in the deshielding region of the purine ring. Such deshielding effects are possible only when χ_{CN} values are greater than ~45°; for torsion angles below this value, all three protons move into regions of increasing shielding (or alternatively smaller deshielding). The crystal structure work (Altona and Sundaralingam, 1972) also indicates an apparent correlation between χ_{CN} and ribose ring conformation; i.e., a low χ_{CN} value, 0° to ~45°, is associated with a favored C3′-endo (*N*) ring, while higher χ_{CN} values, >45°, correlate with a C2′-endo (*S*) ring. This type of rough correlation probably holds in solution; at low adenylate monomer concentrations (<0.1 M), where the ribose ring is predominantly *S*, χ_{CN} is likely to be greater than 45° and H1′, H2′, H3′ experience purine deshieldings. At higher concentrations, where intermolecular stacking is appreciable, there is an $N \rightleftharpoons S$ shift in favor of *N* with an accompanying decrease of χ_{CN}; a lesser deshielding environment thus results for nearby ribose protons. A similar situation holds in the dimer. At room temperature, ApA can be visualized as a limiting case of stacked monomers with *N* ribose conformation and χ_{CN} values at the lower range. The latter, in particular, is supported by the $Ap^-A^+p^-A^+$ structural data which show χ_{CN} magnitudes of 7, 21, and 24° for the three nucleotidyl units. It follows that both sets of ApA ribose 1′, 2′, and 3′ signals will be displaced upfield relative to shieldings in corresponding monomers. A quantitative evaluation of shielding changes ($\Delta\delta$ vs. χ_{CN}) cannot be made in any direct way from measured shift data alone (i.e., δ vs. *T* measurements) but some idea of $\Delta\delta$ magnitudes is possible from adenine isoshielding curves. These show that a rotation of χ_{CN} from ~45 to 0° can produce shift changes of +0.3, +0.1, and +0.2 ppm for H1′, H2′, and H3′, respectively. The shielding increases

[3] It is interesting to note that classical potential energy calculations (Broyde et al., 1974) and extended Hückel MO calculations (Saran and Govil, 1971) show an energy minimum at 80°,20° in ω,ω' maps.

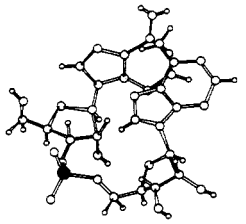

Conformation I

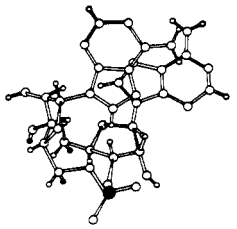

Conformation II

FIGURE 5. Two base-stacked ApA conformations in accord with NMR data. Conformation I is base-stacked (3′ → 5′) anti, C3′-endo, g^-, ω' (330°), ω (320°) $g'g'$, gg, C3′-endo, anti. Conformation II is characterized as base-stacked (though more loosely than in I) with the overall conformation anti, C3′-endo, g^-, ω' (80°), ω(50°) $g'g'$, gg, C3′-endo, anti. In model I the 5′-nucleotidyl unit is located above the 3′ unit and both ribose oxygens are aligned in the same direction. The projection for model II again shows -pA (5′) above Ap- (3′) but with ribose oxygens aligned in opposite directions. The phosphorus atom is denoted by a shaded circle.

when combined with stacking effects give total shift changes closer to those observed experimentally, but any attempt to fix χ_{CN} angles from a comparison of measured and predicted $\Delta\delta(\chi_{CN})$ values is of course questionable. There is, nevertheless, at least a strong likelihood that a substantial part of the (monomer–dimer) shielding changes observed for 1′, 2′, 3′ protons arises from a decrease of χ_{CN} upon dimerization.

Summary of Composite ApA Conformation. A pictorial representation of the composite ApA structures is given in Figure 5. Among the key conformational features clearly established are the following. (i) Both ribose rings exist in a favored *N* (C3′-endo) conformation (60:40, *N*:*S*). This is the conformation found for 5′-AMP, 3′-AMP, and all of the adenylate nucleotides of $Ap^-A^+p^-A^+$ in the crystalline state. It differs markedly, however, from the ring conformation of corresponding monomers in dilute solution where *S* is favored by ~35:65. The difference correlates with the degree of base stacking and glycosidic torsion angle, with the *N* form being favored as stacking increases and $\chi_{CN} \rightarrow 0°$. (ii) Along the ribose phosphate backbone the most preferred conformations are gg (C4′–C5′), $g'g'$ (C5′–O5′), and g^- (C3′–O3′); an analysis of selective shift effects also points to favored rotamers about O5′–P and O3′–P having torsion angles of 320,330° and 80,50° in I and II. The net effect is a highly compact ribose phosphate backbone which permits nucleation of a base-stacked right-hand helical structure in one case, I, and a somewhat looser, but still compact backbone that allows for a stacked loop conformation II. The close similarities between the solution backbone conformations and those found in the crystalline state for several dinucleotides and $Ap^-A^+p^-A^+$, and the observation of minimal changes in rotamer populations in going from monomer to dimer (Table V; Davies and Danyluk, 1974, Table VII), again point to a highly stable dynamical conformation for the backbone. Sarma, in a very recent publication (Lee et al., 1975), has proposed an increase in "conformational purity" of the ribose phosphate backbone with increase in chain length. The addition of nucleotidyl units is presumed to produce a further stabilization of favored rotamers along the backbone. The present dimer and earlier monomer results appear to support such a trend though, as noted above, the changes are near the error limits inherent in rotamer analyses. It should be stressed that the concept of conformational stability or purity evolves from comparisons of backbone conformations in mono- and dinucleotides in crystals and under one set of solution conditions (i.e., pH ~7.0 and μ ~0.05–0.1 M). Whether this stability holds when pD or μ are changed is open to question. Indeed pD measurements (Nelson and Danyluk, unpublished results) show detectable changes in ribose phosphate conformation for most nucleotides over the range pD 1–9. (iii) Base stacking with anti orientations of base and ribose rings in both adenylyl units is confirmed in the present work. A right helical stack is particularly well accommodated by a type I ribose phosphate backbone, while a looser stacking is indicated in the looped conformation II. Though less direct, the present ribose shift data also suggest that base stacking is accompanied by a decrease in glycosidic torsion angle. Since the conformational constraints imposed by a stable ribose–phosphate backbone place a limit on the extent of overlap for the stacked purine rings, a further optimization of the overlap may be facilitated by rotation of the bases about χ_{CN}, i.e., $\chi_{CN} \rightarrow 0°$. At this stage, a further clarification of the role of base–base interactions in fixing backbone conformations and vice versa requires much more detailed knowledge of the relative energetics for all of the conformational processes.

The present NMR results also give a somewhat more detailed insight into base-destacking processes. Previous analyses of spectroscopic data (Ts'o et al., 1969; Hruska and Danyluk, 1968b) for thermally induced (also for solvent- or salt-induced) destacking of dinucleotides, including ApA, generally assumed a simple one-step equilibrium, i.e., $ApA(S) \rightleftharpoons ApA(U)$ with $K_{eq} = N_U/N_S$.

The destacking process itself involved an alteration in base–base separation and/or alignment with the likelihood of ribose involvement indicated by changes of $J_{1'2'}$. Since complete conformational data were unavailable, the nature of stacked and unstacked species was unclear. It now seems likely that the simple one-step equilibrium is incomplete, and we propose that two stacked forms coexist in solution in equilibrium with unstacked ApA. The equilibrium can be represented schematically as follows:

$$\begin{array}{ccc} ApA(I) & \overset{K_I}{\rightleftharpoons} & \\ & & ApA(U) \\ ApA(II) & \underset{K_{II}}{\rightleftharpoons} & \end{array}$$

with ApA(I) being more populated than ApA(II). A further equilibrium between I and II may also exist but *K* for this process is probably less favored since concerted rotation is required about at least two bonds, O5′–P and P–O3′. The conformational nature of ApA(*U*) and, coincidentally, the mechanisms for destacking processes, are difficult to establish, but a tentative model can be pieced together from the available conformational information. As discussed previously, certain regions of the ribose–phosphate backbone,

notably C4′-C5′-O5′ and C3′-O3′, are characterized by unusual stability and these do not change appreciably with temperature (Kondo and Danyluk, 1975). Similarly, both sets of ribose rings and glycosidic torsion angles undergo changes but these again are not sufficient to produce gross changes of base-base orientations. We are thus left with P-O3′ and P-O5′ bonds as likely pivotal points for destacking. As noted earlier destacking in conformation I can readily be accomplished either by an *increase* of $\omega \rightarrow 360°$, or a *decrease* of $\omega' \rightarrow 180°$, or a combination of both. It is tempting then to propose a sequence of events whereby the initial step involves rotation about $\omega(\omega')$ which leads to changes in base-base distances; the unstacking is then accompanied by changes in χ_{CN} (increase) and a shift of ribose conformation in favor of *S* form (C2′-endo). Further measurements using a combination of NMR approaches (CW, pulse) are obviously necessary to establish specifics for destacking or melting mechanisms.

Acknowledgments

The authors are indebted to Drs. H. Crespi and J. J. Katz of the Chemistry Division, Argonne National Laboratory, for supplying fully deuterated algae. We also thank C. F. Ainsworth for assistance in preparing $A\overset{*}{p}A$ and Dr. John F. Thomson for helpful comments on the manuscript.

References

Altona, C., and Sundaralingam, M. (1972), *J. Am. Chem. Soc. 94,* 8205.

Altona, C., and Sundaralingam, M. (1973), *J. Am. Chem. Soc. 95,* 2333.

Arnott, S. (1972), in the Purines-Theory and Experiment (Proceedings of the Jerusalem Symposia IV), Bergmann, E. D., and Pullman, B., ed., Jerusalem, Israel Academy of Sciences and Humanities, p 102.

Blackburn, B. J., Grey, A. A., Smith, I. C. P., and Hruska, F. E. (1970), *Can. J. Chem. 48,* 2866.

Broom, A. D., Schweizer, M. P., and Ts'o, P. O. P. (1967), *J. Am. Chem. Soc. 89,* 3612.

Broyde, S. B., Stellman, S. D., Hingerty, B., and Langridge, R. (1974), *Biopolymers 13,* 1243.

Bush, C. A., and Tinoco, I., Jr. (1967), *J. Mol. Biol. 23,* 601.

Chan, S. I., and Nelson, J. H. (1969), *J. Am. Chem. Soc. 91,* 168.

Danyluk, S. S., and Ezra, F. (1975), unpublished results.

Danyluk, S. S., and Hruska, F. E. (1968), *Biochemistry 7,* 1038.

Davies, D. B., and Danyluk, S. S. (1974), *Biochemistry 13,* 4417.

Davies, D. B., and Danyluk, S. S. (1975), *Biochemistry 14,* 543.

Davis, R. C., and Tinoco, I., Jr. (1968), *Biopolymers 6,* 223.

Evans, F. E., and Sarma, R. H. (1974a), *J. Biol. Chem. 249,* 4754.

Evans, F. E., and Sarma, R. H. (1974b), *Biopolymers 13,* 2117 (and references cited therein).

Giessner-Prettre, C., and Pullman, B. (1970), *J. Theor. Biol. 27,* 87.

Hruska, F. E. (1973), in Conformations of Biological Molecules and Polymers (Proceedings of Jerusalem Symposium V), Bergmann, E. D., and Pullman, B., Ed., Jerusalem, Israel Academy of Sciences and Humanities, p 345.

Hruska, F. E., and Danyluk, S. S. (1968a), *Biochim. Biophys. Acta 157,* 238.

Hruska, F. E., and Danyluk, S. S. (1968b), *J. Am. Chem. Soc. 90,* 3266.

Hruska, F. E., Grey, A. A., and Smith, I. C. P. (1970), *J. Am. Chem. Soc. 92,* 4088.

Hruska, F. E., Wood, D. J., McCaig, T. N., Smith, A. A., and Holy, A. (1974), *Can. J. Chem. 52,* 497.

Hruska, F. E., Wood, D. J., Mynott, R. J., and Sarma, R. H. (1973), *FEBS Lett. 31,* 153.

Kan, L. S., Barrett, J. C., Miller, P. S., and Ts'o, P. O. P. (1973), *Biopolymers 12,* 2225.

Kim, S.-H., Berman, H. M., Seeman, N. C., and Newton, M. D. (1973), *Acta Crystallogr. Sect. B 29,* 703.

Kondo, N. S., and Danyluk, S. S. (1972), *J. Am. Chem. Soc. 94,* 5121.

Kondo, N. S., and Danyluk, S. S. (1974), Fifth International Symposium on Magnetic Resonance, Bombay, Jan 1974, Abstr. 14A48.

Kondo, N. S., and Danyluk, S. S. (1975), unpublished results.

Kondo, N. S., Ezra, F., and Danyluk, S. S. (1975), *FEBS Lett. 53,* 213.

Kondo, N. S., Leung, A., and Danyluk, S. S. (1973), *J. Labelled Compd. 9,* 497.

Lee, C.-H., Evans, F. E., and Sarma, R. H. (1975), *FEBS Lett. 63,* 106.

Lohrmann, R., and Khorana, H. G. (1964), *J. Am. Chem. Soc. 86,* 4188.

Perahia, D., Pullman, B., and Saran, A. (1974), *Biochim. Biophys. Acta 340,* 299.

Remin, M., and Shugar, D. (1972), *Biochem. Biophys. Res. Commun. 48,* 636.

Rosenberg, J. M., Seeman, N., Kim, S-H., Suddath, F. L., Nicholas, H. B., and Rich, A. (1973), *Nature (London), New Biol. 243,* 150.

Saran, A., and Govil, G. (1971), *J. Theor. Biol. 33,* 407.

Sarma, R. H., and Mynott, R. J. (1973), *J. Am. Chem. Soc. 95,* 1641.

Schirmer, R. E., Davis, J. P., Noggle, J. H., and Hart, P. A. (1972), *J. Am. Chem. Soc. 94,* 2561.

Schweizer, M. P., Broom, A. D., Ts'o, P. O. P., and Hollis, D. P. (1968), *J. Am. Chem. Soc. 90,* 1042.

Schweizer, M. P., Chan, S. I., and Ts'o, P. O. P. (1965), *J. Am. Chem. Soc. 87,* 5241.

Stellman, S. D., Hingerty, B., Broyde, S. B., Subramanian, E., Sato, T., and Langridge, R. (1973), *Biopolymers 12,* 2731.

Suck, D., Manor, P. C., Germain, G., Schwalbe, C. H., Weimann, G., and Saenger, W. (1973), *Nature (London), 246,* 161.

Sundaralingam, M. (1969), *Biopolymers 7,* 821.

Sundaralingam, M. (1973), in Conformations of Biological Molecules and Polymers (Proceedings of the Jerusalem Symposium V), Bergmann, E. D., and Pullman, B., Ed., Jerusalem, Israel Academy of Sciences and Humanities, p 417.

Sussman, J., Seeman, N., Kim, S.-H., and Berman, H. (1972), *J. Mol. Biol. 66,* 403.

Tewari, R., Nanda, R. K., and Govil, G. (1974), *J. Theor. Biol. 46,* 229.

Ts'o, P. O. P. (1974), Basic Principles in Nucleic Acid Chemistry, Vol. II, Ts'o, P. O. P., Ed., New York, N.Y., Academic Press, Chapter 5.

Ts'o, P. O. P., Kondo, N. S., Schweizer, M. P., and Hollis, D. P. (1969), *Biochemistry 8,* 997.
Tsuboi, M., Takahiski, S., Kyogoku, Y., Hayatsu, H., Ukita, T., and Kainosho, M. (1969), *Science 166,* 1504.
Warshaw, M. M., and Tinoco, I., Jr. (1965), *J. Mol. Biol. 13,* 54.
Yathindra, N., and Sundaralingam, M. (1974), *Proc. Natl. Acad. Sci. U.S.A., 71,* 3325.

Conformational Studies of Peptide *Cyclo*-(D-Val-L-Pro-L-Val-D-Pro)$_3$, a Cation-Binding Analogue of Valinomycin†

Donald G. Davis,*,‡ B. F. Gisin, and D. C. Tosteson§

ABSTRACT: The solution conformation of *cyclo*-[D-Val-L-Pro-L-Val-D-Pro]$_3$ (PV) and its alkali-metal ion complexes was investigated by proton nuclear magnetic resonance spectroscopy. It is concluded that the cation complexes of PV have S_6 symmetry and are essentially isostructural with the K complex of valinomycin. In contrast to valinomycin, the Li- and Na-PV complexes are stable in methanol and have dissociation rate constants that are several orders of magnitude slower than the corresponding valinomycin complexes. Also in contrast to valinomycin, free PV exists in two different conformational states which interconvert at very slow rates ($\ll 1$ s^{-1}). One of these conformers has S_6 symmetry and is structurally similar to that of the cation complexes. The other species, which has lower symmetry than S_6, is the more stable conformer. Depending upon concentration and solvent polarity, the latter represents between 50 and 75% of the total mixture. It is proposed that PV may have a higher affinity for cations than valinomycin because of its higher potential energy in the uncomplexed state.

The facilitated and selective transport of cations across membranes by cyclic antibiotics such as valinomycin has been studied extensively (Läuger, 1972; Haydon and Hladky, 1972; Grell et al., 1972; Eisenman et al., 1973). Structural investigations show as well that the cation-carrier function of valinomycin is a consequence of its conformational properties. For example, the conformation of the K-valinomycin molecule provides for a polar, cation-binding site in which the ion is shielded from the low dielectric interior of the membrane by an exterior surface studded with hydrocarbon side chains (Ivanov et al., 1969; Pinkerton et al., 1969). This conformation, which is the basis for the ion-carrier activity of valinomycin, appears to be extremely sensitive to changes in the primary structure of the molecule (Merrifield et al., 1969; Ovchinnikov et al., 1972).

To investigate further the relationship between structure and function in these macrocyclic compounds and to test generalizations that have been proposed from studies on valinomycin, a cyclic dodecapeptide analogue of valinomycin was synthesized (Gisin and Merrifield, 1972). This compound, designated here as PV,[1] has the formula *cyclo*-[D-Val-L-Pro-L-Val-D-Pro]$_3$ and is related to valinomycin by the substitution of D- and L-prolines for D-hydroxyisovalerate and L-lactate residues, respectively. This substitution not only preserves the threefold periodicity of the sequence and the sequential order of optical isomers, but also restricts H-bond donors to the amide protons of the valines. In valinomycin, these latter constraints are thought to be important requirements for the formation and stabilization of the series of alternating β turns which characterize the bracelet-like secondary structure of the K ion complex (Ohnishi and Urry, 1971; Ovchinnikov et al., 1972).

Although the functional properties of PV resemble those of valinomycin qualitatively, PV is substantially different when compared to valinomycin in quantitative terms. Estimates of the affinities of PV for alkali metal ions in single and two phase bulk systems are at least 10^3 times larger than those for valinomycin (Gisin and Davis, 1973). On the other hand, when compared in terms of the concentrations required to produce a given membrane conductance in lipid-bilayer experiments, PV is less potent than valinomycin by a factor of 10^3 (Ting-Beal et al., 1974). The latter appears to be somewhat paradoxical in light of the higher cation affinities of PV and it points to the need for further experimental information about the structural properties of this peptide.

This paper deals with a proton nuclear magnetic resonance (^{1}H NMR) investigation into the solution conformations of PV and its complexes with alkali metal ions. Infor-

† From the Department of Physiology and Pharmacology, Duke University Medical Center, Durham, North Carolina 27710 (D.G.D., D.C.T., and B.F.G.), and the Rockefeller University, New York, N.Y. 10021 (B.F.G.). *Received July 22, 1975.* This work was supported by Research Grant HL12157 from the National Institutes of Health. The MPC 250 spectrometer facility (CMU) is supported by National Institutes of Health Grant RR-00292.
‡ National Institutes of Health Special Fellow FO 3GM52677-02.
* Author to whom to address correspondence. Present address: Department of Chemistry, Adelphi University, Garden City, New York 11530.
§ Present address: Division of Biological Sciences, Pritzker School of Medicine, University of Chicago, Chicago, Illinois 60637.

[1] Abbreviations used are: PV, *cyclo*-[D-Val-L-Pro-L-Val-D-Pro]$_3$; TNC, 2,4,6-trinitro-*m*-cresolate.